

UCT-TP-260/03  
February 2003

## Electromagnetic nucleon form factors from QCD sum rules

H. Castillo <sup>(a);(b)</sup>, C. A. Dominguez <sup>(c)</sup>, M. Loewe <sup>(a)</sup>

(a) Facultad de Física, Pontificia Universidad Católica de Chile, Casilla 306, Santiago 22, Chile.  
(b) Departamento de Ciencias, Pontificia Universidad Católica del Perú, Apartado 1761, Lima, Perú.  
(c) Department of Physics, University of Cape Town, Rondebosch 7701, South Africa.

### Abstract

The electromagnetic form factors of the nucleon, in the space-like region, are determined from three-point function Finite Energy QCD Sum Rules. The QCD calculation is performed to leading order in perturbation theory (in the chiral limit), and to leading order in the non-perturbative power corrections, proportional to the quark condensate. The results are in good agreement with the data for both the proton and neutron form factors in the currently accessible experimental region of momentum transfers.

The asymptotic behaviour of the electromagnetic form factors of the nucleon have been studied in perturbative QCD, together with QCD sum rule estimates of the nucleon wave functions [1]. Comparison with data is difficult due to the extreme asymptotic nature of these results. In addition, these wave functions are affected by some unavoidable model dependency. In view of this, it is desirable to attempt a field theoretic QCD determination in a region of experimentally accessible momentum transfers, and without any reference to the concept of a wave function.

In this note we determine the electromagnetic nucleon form factors, in a wide range of (space-like) momentum transfers, in the framework of three-point function Finite Energy QCD sum rules. As is well known by now, this technique is based on the Operator Product Expansion (OPE) of current correlators at short distances, and on the notion of quark-hadron duality [2]. Analyticity and dispersion relations connect then the QCD information in the OPE with hadronic parameters entering the corresponding spectral functions. We compute the QCD correlator to leading order in perturbative QCD, in the chiral limit ( $m_u = m_d = 0$ ), and include the leading order non-perturbative power correction proportional to the quark-condensate.

We begin by considering the following three-point function (see Fig. 1)

$$\langle p^2; p^0; Q^2 \rangle = i^2 \int d^4x d^4y e^{i(p^0 x - q y)} \bar{u}(T f_N(x)) J_{EM}^N(y) u(0) i; \quad (1)$$

where  $Q^2 = (p^0 - p)^2 \neq 0$  is fixed, and

$$f_N(x) = \epsilon_{abc} u^a(x) (C - \gamma^5) u^b(x) \bar{u}^c(x) \quad (2)$$

is an interpolating current with nucleon (proton) quantum numbers; the neutron case will be discussed at the end. In Eq.(1),  $J_{EM}^N$  is the electromagnetic current

$$J_{EM}^N(y) = \frac{2}{3} u(y) \bar{u}(y) - \frac{1}{3} \bar{d}(y) d(y); \quad (3)$$

The current Eq.(2) couples to a nucleon of momentum  $p$  and polarization  $s$  according to

$$h \bar{u}(0) J_N(p; s) i = f_N u(p; s); \quad (4)$$

where  $u(p; s)$  is the nucleon spinor, and  $f_N$ , the current-nucleon coupling, is a phenomenological parameter a priori unknown. This parameter can be estimated, e.g. using QCD sum rules for a two-point function involving the currents  $f_N$  [3]. In this case one can determine the nucleon mass, as well as the coupling  $f_N$ .

Concentrating first on the hadronic sector, and inserting a one-particle nucleon state in the three-point function (1) brings out the nucleon form factors  $F_1(q^2)$ , and  $F_2(q^2)$ , defined as

$$h k_1 s_1 J_{EM}^N(0) k_2 s_2 i = u_N(k_1; s_1) F_1(q^2) + \frac{i}{2M_N} F_2(q^2) q \cdot u_N(k_2; s_2); \quad (5)$$

where  $q^2 = (k_2 - k_1)^2$ , and  $\mu$  is the anomalous magnetic moment in units of nuclear magnetons ( $\mu_p = 1.79$  for the proton, and  $\mu_n = 1.91$  for the neutron). The form factors  $F_{1,2}(q^2)$  are related to the electric and magnetic (Sachs) form factors  $G_E(q^2)$ , and  $G_M(q^2)$ , measured in elastic electron-proton scattering experiments, according to

$$G_E(q^2) = F_1(q^2) + \frac{q^2}{(2m)^2} F_2(q^2); \quad (6)$$

$$G_M(q^2) = F_1(q^2) + \mu F_2(q^2); \quad (7)$$

where  $G_E^p(0) = 1$ ,  $G_M^p(0) = 1 + \mu_p$  for the proton, and  $G_E^n(0) = 0$ ,  $G_M^n(0) = \mu_n$  for the neutron. Next, the hadronic spectral function is obtained after inserting a complete set of nucleonic states in (1), and computing the discontinuity in the complex  $p^2 = s, p^0 = s^0$  plane. For  $s; s^0 < 2.1 \text{ GeV}^2$ , i.e. below the Roper resonance, one can safely approximate the hadronic spectral function by the single-particle nucleon pole, followed by a continuum with thresholds  $s_0$  and  $s_0^0$  ( $s_0; s_0^0 > M_N^2$ ). This hadronic continuum is expected to coincide numerically with the perturbative QCD (PQCD) spectral function (local duality). This procedure is standard in QCD sum rule applications, and leads to

$$\begin{aligned} \text{Im} \quad (s; s^0; Q^2)_{\text{HAD}} &= \frac{2}{N} (s - M_N^2) (s^0 - M_N^2) \\ &\quad (F_1(q^2) \not{p}^0 \not{p} + M_N (\not{p}^0 + \not{p}) + M_N^2) \\ &\quad + \frac{i}{2M_N} F_2(q^2) \not{p}^0 \not{p} + M_N (\not{p}^0 + \not{p}) + M_N^2 \quad q = (s_0 - s) \\ &\quad + \text{Im} \quad (s; s^0; Q^2)_{\text{PQCD}} (s - s_0); \end{aligned} \quad (8)$$

where we have set  $s_0 = s_0^0$  for simplicity.

Turning to the QCD sector, the three-point function (1) to leading order in perturbative QCD, and in the chiral limit, is given by

$$\begin{aligned} (p^2; p^0; Q^2) &= 16 \int d^4x \int d^4y e^{i(p^0 x - q^0 y)} \text{Tr} \left[ \frac{d^4 k_1}{(2\pi)^4} \frac{\not{k}_1}{k_1^2} e^{i k_1 \cdot (x - y)} \right. \\ &\quad \left. \frac{d^4 k_2}{(2\pi)^4} \frac{\not{k}_2}{k_2^2} e^{i k_2 \cdot y} \right] \int d^4x \int d^4y e^{i(p^0 x - q^0 y)} \text{Tr} \left[ \frac{d^4 k_3}{(2\pi)^4} \frac{\not{k}_3}{k_3^2} e^{i k_3 \cdot x} \right. \\ &\quad \left. \frac{d^4 k_4}{(2\pi)^4} \frac{\not{k}_4}{k_4^2} e^{i k_4 \cdot x} \right] \int d^4x \int d^4y e^{i(p^0 x - q^0 y)} \text{Tr} \left[ \frac{d^4 k_4}{(2\pi)^4} \frac{\not{k}_4}{k_4^2} e^{i k_4 \cdot x} \right. \\ &\quad \left. \frac{d^4 k_1}{(2\pi)^4} \frac{\not{k}_1}{k_1^2} e^{i k_1 \cdot (x - y)} \right] \int d^4x \int d^4y e^{i(p^0 x - q^0 y)} \text{Tr} \left[ \frac{d^4 k_2}{(2\pi)^4} \frac{\not{k}_2}{k_2^2} e^{i k_2 \cdot y} \right. \\ &\quad \left. \vdots \right] \end{aligned} \quad (9)$$

After computing the traces and performing the momentum space integrations, Eq.(9) involves several Lorentz structures analogous to those entering the hadronic spectral function Eq. (8). Before invoking

duality one needs to choose a particular Lorentz structure present in both (8) and (9). A convenient choice turns out to be  $\not{p}^0 \not{p}$ , which allows to project  $F_1(q^2)$ , as this structure does not appear multiplying  $F_2(q^2)$  in Eq.(8). An additional advantage of this choice is that the quark condensate contribution, to be discussed later, does not involve the structure  $\not{p}^0 \not{p}$ , on account of vanishing traces. Hence,  $F_1(q^2)$  will be dual only to the PQCD expression. It must be pointed out that the PQCD spectral function contains the structure  $\not{p}^0 \not{p}$  explicitly, as well as implicitly, i.e. there are terms proportional to this structure which are generated only after momentum space integration.

After a very lengthy calculation, the imaginary part of Eq.(9) is given by

$$\text{Im} \quad (s; s^0; Q^2) = \frac{4}{(2)^8} (3_1 + 4_2 - 3_3) (\not{p}^0 \not{p}) + \dots; \quad (10)$$

where

$$1 = \frac{6}{2} \frac{0}{Q^2 + s - s^0} \frac{Q^4 + 2Q^2s + s^2 - 2ss^0 - s^0}{Q^4 + (s - s^0)^2 + 2Q^2(s + s^0)} \frac{1}{A}; \quad (11)$$

$$2 = \frac{8}{6} \frac{\not{p}^0}{Q^2 + 3s - 3s^0} \frac{(Q^2 + s)^3 (2Q^2 + 3s) + 3Q^6 - 5Q^2s^2 - 4s^3 - s^0}{3Q^4 + (s - s^0)^2 + 2Q^2(s + s^0)} \frac{1}{\not{p}}; \\ + \frac{h}{(3Q^2 - 4s)(Q^2 + 3s)s^0 + 7Q^2s^0 + 3s^0} \frac{i^9}{3Q^4 + (s - s^0)^2 + 2Q^2(s + s^0)} \frac{1}{\not{p}}; \quad (12)$$

$$3 = \frac{6}{72} \frac{23Q^2 + 18(s + s^0)}{Q^4 + (s - s^0)^2 + 2Q^2(s + s^0)} + \frac{6}{72} \frac{h}{Q^4 + (s - s^0)^2 + 2Q^2(s + s^0)} \frac{1}{\not{p}} \\ + \frac{23Q^2 - 18s - Q^2 + s^5 + Q^2 + s^3 - 133Q^4 - 169Q^2s + 108s^2 - s^0}{Q^4 + (s - s^0)^2 + 2Q^2(s + s^0)} \\ + \frac{2160Q^8 + 6Q^6s + 3Q^4s^2 + 40Q^2s^3 - 117s^4 - s^0}{Q^4 + (s - s^0)^2 + 2Q^2(s + s^0)} \\ + \frac{2205Q^6 - 61Q^4s - 122Q^2s^2 + 108s^3 - s^0}{Q^4 + (s - s^0)^2 + 2Q^2(s + s^0)} \\ + \frac{295Q^4 - 37Q^2s - 54s^2 - s^0 + 113Q^2 - 36s - s^0 - 18s^0}{Q^4 + (s - s^0)^2 + 2Q^2(s + s^0)} \frac{i}{\not{p}}; \quad (13)$$

Equation (11) corresponds to the terms containing  $\not{p}^0 \not{p}$  explicitly, and Eqs.(12)–(13) to the implicit case. The spectral function (10) contains additional terms proportional to other (independent) Lorentz

structures, which are not given. Collecting all three term s in (10) leads to

$$\begin{aligned}
\text{Im} \quad (s; s^0; Q^2) = & \frac{323Q^2 + 378(s - s^0)}{4608^2} + \frac{1}{4608^2 Q^4 + (s - s^0)^2 + 2Q^2(s + s^0)^2} \\
& h \quad 323Q^{12} Q^{10} (1993s + 1237s^0) \quad 10Q^8 (512s^2 + 323ss^0 + 134s^0) \\
& + Q^6 (-7010s^3 + 1188ss^2 + 550s^3) \\
& + Q^4 (-5395s^4 + 7010s^3s^0 + 2610s^2s^0 + 3146ss^3 + 2165s^4) \\
& Q^2 (s - s^0)^2 (2213s^3 - 2859s^2s^0 - 3099ss^2 - 1567s^3) \\
& 378(s - s^0)^4 (s^2 - 2ss^0 - s^0) \quad \frac{1}{p^0} \quad p + \dots \quad (14)
\end{aligned}$$

The next step is to invoke (global) quark-hadron duality, according to which the area under the hadronic spectral function equals the area under the corresponding QCD spectral function. The integrals in the complex energy plane may involve any analytic integration kernel; this leads to different kinds of QCD sum rules, e.g. Laplace (negative exponential kernel), Finite Energy Sum Rules (FESR) (power kernel), etc. We choose the latter, as they have the advantage of being organized according to dimensionality (to leading order in gluonic corrections to the vacuum condensates). In this case the leading dimension FESR is

$$\int_0^{s_0} ds \int_0^{s_0} ds^0 \text{Im} (s; s^0; Q^2) \underset{\text{HAD}}{\mathcal{J}} = \int_0^{s_0} ds \int_0^{s_0} ds^0 \text{Im} (s; s^0; Q^2) \underset{\text{QCD}}{\mathcal{J}} : \quad (15)$$

The integration region, shown in Fig. 2, has been chosen as a triangle; the main contribution being that of region I, and the area included from regions II and III tends to compensate the excluded regions. Other choices, e.g. rectangular regions, lead to similar results, as discussed in [5]-[6]. After performing the integrations, one finally obtains

$$\begin{aligned}
F_1(Q^2) = & \frac{2s_0 - 96Q^6 + 297Q^4s_0 + 158Q^2s_0^2 - 112s_0^3}{9216^4 (Q^2 + 2s_0)^2} \\
& + \frac{3 \ln(\frac{Q^2}{Q^2 + 2s_0}) Q^2 + 2s_0 - 32Q^6 + 67Q^4s_0 + 7Q^2s_0^2 - 21s_0^3}{9216^4 (Q^2 + 2s_0)^2} ; \quad (16)
\end{aligned}$$

where one can recognize the standard logarithmic singularity arising from the chiral limit.

We now turn to the extraction of  $F_2(q^2)$ , and consider the leading order non-perturbative power correction to the OPE, in this case given by the quark condensate contribution. It turns out that the contribution involving the up-quark condensate vanishes (on account of vanishing traces), leaving only the piece

proportional to  $hddi$ . The three-point function (1) becomes (see Fig. 3)

$$\begin{aligned} hqqi(p^2; p^0; Q^2) &= i \frac{hddi}{3(2)^4} \int d^4k \frac{\text{Tr} [k \cdot (k \cdot q) \cdot (k \cdot p^0)]}{(k \cdot q)^2 (k \cdot p^0)^2 k^2} \\ &= \int d^4k \frac{\text{Tr} [k \cdot (k \cdot p^0)]}{k^2 (k \cdot p^0)^2 q^2} (q \cdot k) + \int d^4k \frac{\text{Tr} [k \cdot (k \cdot p)]}{k^2 (k \cdot p)^2 q^2} (q \cdot k) : \end{aligned} \quad (17)$$

Our choice of Lorentz structure in this case is  $q \cdot k$ , which appears in Eq.(17), as well as in Eq.(8) where it multiplies  $F_2(q^2)$ , but not  $F_1(q^2)$ . In fact, after some algebra

$$\text{Im}_{QCD}^{hddi}(s; s^0; Q^2) = \frac{hddi}{3} \gtrless \frac{Q^2 s^0 Q^2 + 3s + s^0}{Q^4 + (s - s^0)^2 + 2Q^2 (s + s^0)} \stackrel{8}{\gtrless} + \frac{1}{(2)} \frac{(s^0 - s)}{Q^2} \stackrel{9}{\gtrless} q \cdot k + \dots; \quad (18)$$

and

$$\text{Im}_{HAD}(s; s^0; Q^2) = F_2(Q^2) \frac{p}{2} \frac{s^0}{M_N} + M_N q \cdot k + \dots \quad (19)$$

After substituting the above two spectral functions in the FESR Eq. (15), and performing the integrations one obtains

$$F_2(Q^2) = \frac{hddi}{24 p M_N} \frac{2s_0 Q^2 + s_0 + Q^2 Q^2 + 2s_0 \ln(\frac{Q^2}{Q^2 + 2s_0})}{Q^2 + 2s_0} : \quad (20)$$

The results for the form factors  $F_{1,2}(q^2)$ , Eqs. (16) and (20), involve the free parameters  $M_N$  and  $s_0$ . From QCD sum rules for two-point functions involving the nucleon current (2) it has been found [2]-[3] that  $M_N \approx (1-3) \cdot 10^2 \text{ GeV}^3$ , and  $\frac{p}{s_0} \approx (1:1-1:5) \text{ GeV}$ . The higher values of  $M_N$  and  $s_0$  come from Laplace sum rules [3], and the lower values are from a FESR analysis [4] which yields the relation  $s_0^3 = 192 \cdot \frac{4}{M_N^2}$ . Additional constraints on these parameters follow, in the present analysis, from the asymptotic behaviour of  $F_1(q^2)$ , and the normalization of  $F_2(q^2)$  at  $q^2 = 0$ . In fact, from Eq.(16) it follows that

$$\lim_{Q^2 \rightarrow 1} Q^4 F_1(Q^2) = \frac{11 s_0^5}{2560 \cdot \frac{4}{M_N^2}} ; \quad (21)$$

and from Eq.(20) one finds

$$F_2(0) - 1 = \frac{hddi s_0^2}{12 \cdot \frac{2}{p} M_N \cdot \frac{2}{N}} : \quad (22)$$

Using  $hddi \approx 0.014 \text{ GeV}^3$ , and taking  $Q^4 F_1(Q^2) \approx 1.0 \text{ GeV}^4$  as a representative asymptotic value, as indicated by the experimental data [7] in the region  $Q^2 \approx 10-30 \text{ GeV}^2$ , the above two equations lead to  $s_0 \approx 1.2 \text{ GeV}^2$ , and  $M_N \approx 10^2 \text{ GeV}^3$ , in very good agreement with results from the two-point function analysis [3], [4]. It should be noticed that the resulting value of  $s_0$  is only mildly dependent on the assumed asymptotic value of the left hand side of Eq. (21), as the determining equation involves  $s_0^3$ . Numerically,  $s_0$  is well below the Roper resonance peak, thus justifying the model used for the hadronic spectral function, Eq.(8).

In any case, treating  $s_0$  and  $N$  as free parameters, and performing a least-squares fit to the data on the proton magnetic form factor  $G_M(Q^2)$ , leads to  $s_0 = 1.21 \text{ GeV}^2$ , and  $N = 2.1 \times 10^{-2} \text{ GeV}^3$ , in line with the values discussed above. The predicted form factor is shown in Fig.4 (solid line) together with the experimental data [7]. The result from the empirical dipole approximation

$$G_M^D(Q^2) = \frac{1 + \frac{p}{Q^2}}{(1 + \frac{Q^2}{0.71})^2}; \quad (23)$$

with  $Q^2$  expressed in  $\text{GeV}^2$ , overlaps with the solid line in Fig. 4 to the extent that the differences cannot be resolved. As may be appreciated from Fig. 4, the agreement of this QCD sum rule determination with the data is quite satisfactory.

Considering now the neutron form factors, one needs to make the change  $u \rightarrow d$  in Eq.(2). The perturbative QCD spectral function, Eq.(10), involves now the combination  $(u_3 - u_2)$ . After using the FESR Eq.(15) it turns out that  $F_1(Q^2)$  for the neutron is numerically very small and consistent with zero, except near  $Q^2 = 0$  where it diverges in the chiral limit. In fact,  $0 \leq Q^4 F_1(Q^2) \leq 0.05 \text{ GeV}^4$  in the range  $0 \leq Q^2 \leq 30 \text{ GeV}^2$ . This smallness of the neutron electric form factor provides a nice self-consistency check of the method. The Sachs form factors of the neutron,  $G_E(Q^2)$  and  $G_M(Q^2)$ , which are then basically determined by  $F_2(Q^2)$ , turn out to be almost identical to the dipole parametrization for  $Q^2 > 5 \text{ GeV}^2$ . This agrees with the experimental data, measured up to about  $Q^2 \leq 10 \text{ GeV}^2$ , although the experimental errors are rather large [8].

We comment, in closing, on the next-to-leading order (NLO) contributions to the three-point function, Eq.(1), which were not considered here. On the perturbative sector we expect the gluonic corrections to be small, on account of the extra loop involved, plus the overall factor of  $s$ . The NLO power correction in the Operator Product Expansion involves the gluon condensate. This contribution is also expected to be small, as it contains one more loop with respect to the leading quark condensate term. In addition, further suppression of about one order of magnitude would arise from numerical factors involved in the contraction of the gluon field tensors. On the hadronic sector, the standard single-particle pole plus continuum model adopted for the spectral function is well justified, *a posteriori*, from the resulting value of the continuum threshold  $s_0$ , well below the Roper resonance.

## References

- [1] For a review see e.g. V.L. Chemeris, I.R. Zhitnitsky, Phys. Rep. 112 (1984) 173.
- [2] For a recent review see e.g. P. Colangelo, A. Khodjamirian, in "At the frontiers of particle physics, Handbook of QCD, Vol. 3, 1495, M. A. Shifman, ed., World Scientific, Singapore, 2001).
- [3] For a review see e.g. L.J. Reinders, H. Rubinstein, S. Yazaki, Phys. Rep. 127 (1985) 1.

[4] C A .D om inguez, M .Loewe, Z .Phys.C 58 (1993) 273.

[5] B L .Io e, Nucl.Phys.B 188 (1981) 817; E :B 191 (1981) 591.

[6] C A .D om inguez, M .Loewe, J.S.Rozow sky, Phys.Lett.B 335 (1994) 506.

[7] T .Jansens et al, Phys. Rev. 142 (1965) 922; W .Bartel et al, Phys. Lett. B 33 (1970) 245; C H .Berger et al, Phys. Lett. B 35 (1971) 87; F .Borkowski et al, Nucl. Phys. B 93 (1975) 461; R G .A mold et al, Phys. Rev. Lett. 57 (1986) 174; R C .W alker et al, Phys. Lett. B 234 (1989) 353.

[8] M .G ari, W .K rum peln ann, Z .Phys.A 322 (1985) 689.

### F igure C options

F igure 1. The three-point function, Eq. (1), to leading order in perturbative QCD .

F igure 2. Triangular and rectangular integration regions of the F inite Energy Sum Rules, Eq. (15).

F igure 3. Non-vanishing terms proportional to the down-quark condensate, Eq. (17).

F igure 4. Experimental data on  $G_M^p(Q^2)$  [7], together with the result of this determination (solid line). The dipole  $t$ , Eq. (23), overlaps almost completely with the solid line.

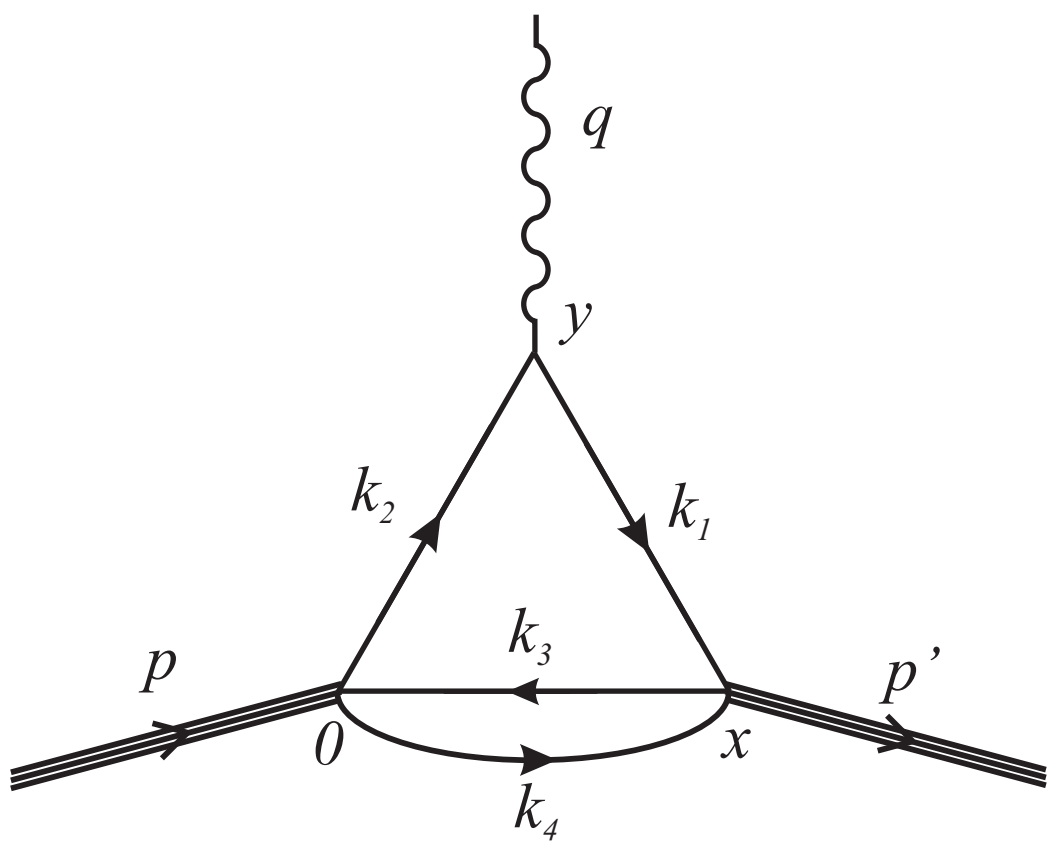


Figure 1:

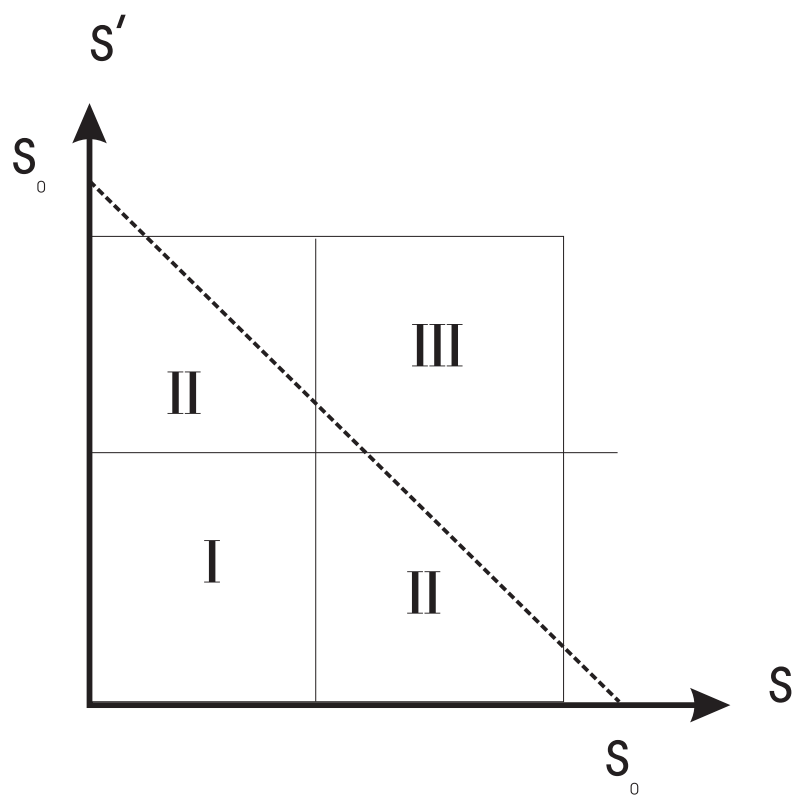


Figure 2:

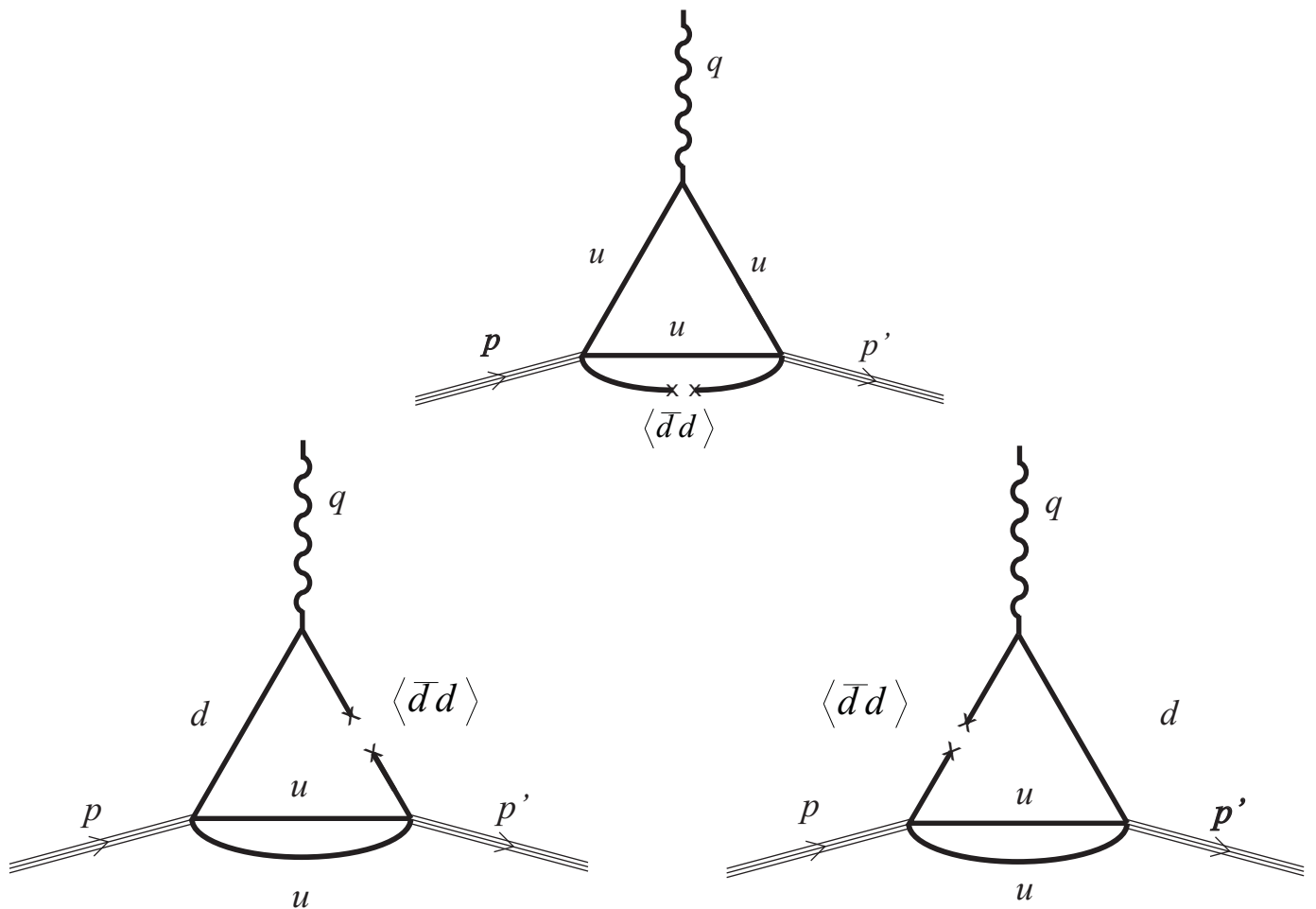


Figure 3:

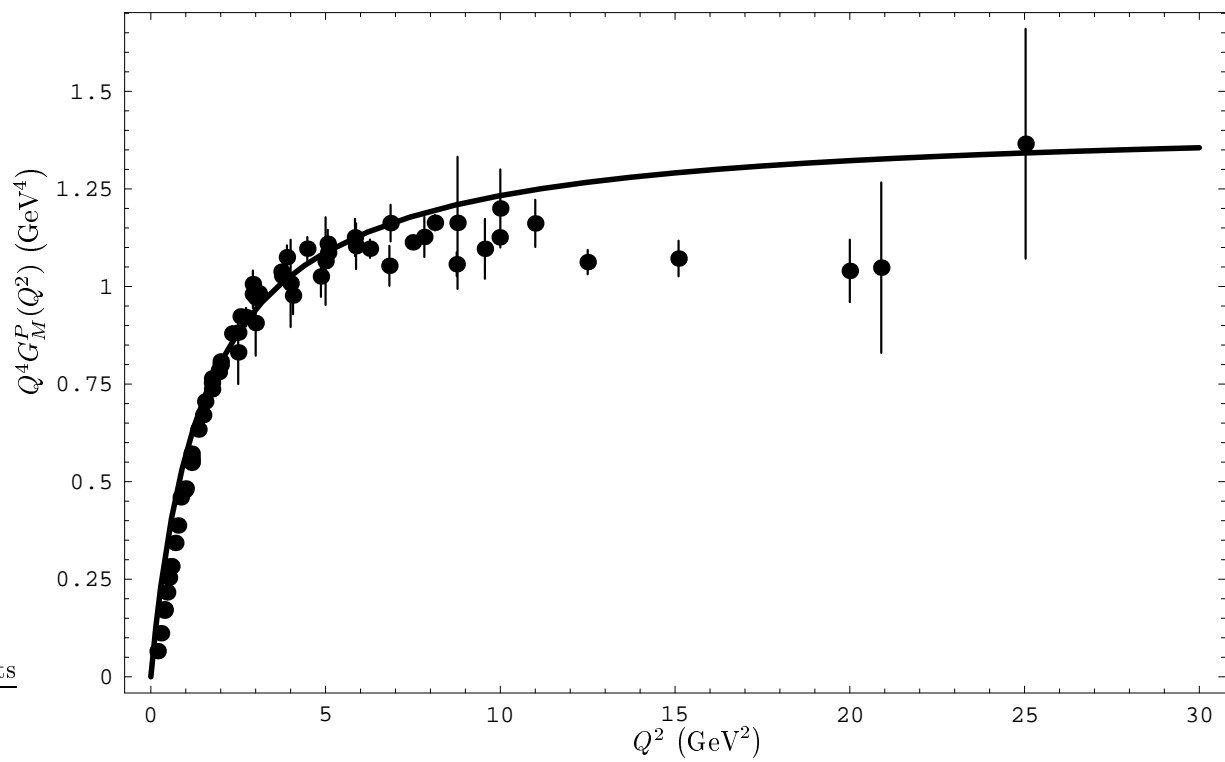


Figure 4: